# Common Metal Ion Coordination in LIM Domain Proteins†

Jessica L. Kosa,‡,§ James W. Michelsen,∥ Heather A. Louis,∥ Jay I. Olsen,⊥ Darrell R. Davis,§,⊥ Mary C. Beckerle,*,∥ and Dennis R. Winge*,‡,§

*Departments of Medicine, Biochemistry, Biology, and Medicinal Chemistry, University of Utah, Salt Lake City, Utah 84132*

*Received August 12, 1993; Revised Manuscript Received October 29, 1993*®

ABSTRACT: The LIM motif is a cysteine- and histidine-rich sequence that was first identified in proteins involved in control of gene expression and cell differentiation. In order to characterize structural features of the LIM domain, we have carried out biophysical studies on two polypeptides that display LIM domains: the cysteine-rich intestinal protein (CRIP) and a fragment of the cysteine-rich protein (CRP). Bacterial expression vectors were constructed for the intact CRIP molecule and the C-terminal half of CRP, designated LIM2, such that each expressed protein contained a single LIM domain. Both proteins were recovered as soluble, Zn(II)-containing proteins. The metal coordination properties of these two distinct LIM domain proteins were highly similar, suggesting that a common structural architecture may exist in LIM domain proteins. Both proteins exhibit a maximum of two tetrahedrally bound Zn(II) ions per molecule. Electronic spectroscopy of Co(II) complexes and $^{113}Cd$ NMR of Cd(II) complexes of CRIP and LIM2 revealed a similar ligand field pattern with one tetrathiolate ($S_4$) site and one $S_3N_1$ site for divalent metal ions. The nitrogen ligand was shown to arise from a histidyl imidazole by heteronuclear multiple quantum coherence NMR. The eight conserved residues within the LIM domains of CRIP and LIM2 include seven cysteines and one histidine. It is likely that these conserved residues generate the $S_4$ and $S_3N_1$ Zn(II)-binding sites. Metal binding to the two sites within a single LIM domain is sequential, with preferential occupancy of the $S_4$ site. Slow metal ion exchange occurs between sites within an LIM domain, and metal exchange with exogenous metal ions is observed, with exchange at the $S_3N_1$ site being kinetically more facile. In the absence of metal binding both proteins appear to be substantially unfolded. Metal binding stabilizes a tertiary fold containing appreciable secondary structural elements. The common metal ion coordination in CRIP and LIM2 suggests that the LIM motif may constitute a structural module with conserved features.

The LIM motif is a cysteine-rich sequence found in a number of proteins that appear to be important for regulation of cell function during development. The LIM motif [$CX_2CX_{16-23}HX_2CX_2CX_{16-21}CX_{2-3}$(C,H,D)] was first defined in three proteins, Lin-11, Isl-1, and Mec-3 (Freyd et al., 1990; Karlsson et al., 1990), from which the term "LIM" is derived (Freyd et al., 1990). Since the initial description of the LIM motif, a number of other proteins that exhibit this sequence motif have been identified. Seven of the known LIM domain proteins also exhibit homeodomains; these include Lin-11, which is required for an asymmetric cell division essential for vulva formation in *Caenorhabditis elegans* (Freyd et al., 1990); Isl-1 and Lmx-1, two insulin gene enhancer binding proteins (Karlsson et al., 1990; German et al., 1992); Mec-3, a *C. elegans* protein required for touch cell neuron differentiation (Way & Chalfie, 1988); Xlim-1, a *Xenopus* protein implicated in pattern formation during gastrulation (Taira et al., 1992); apterous, a *Drosophila* protein required for development of embryonic muscle (Bougouin et al., 1992; Cohen et al., 1992); and LH-2, a mammalian protein important for differentiation of B-lymphocytes (Xu et al., 1993).

In addition to the LIM homeodomain proteins, the LIM motif has also been identified in a collection of proteins that lack obvious DNA-binding domains. The simplest of these is the cysteine-rich intestinal protein (CRIP), which contains a single LIM domain (Birkenmeier & Gordon, 1986). CRIP is a developmentally-regulated intestinal protein (Birkenmeier & Gordon, 1986) that is believed to function in intestinal zinc transport (Hempe & Cousins, 1991). Members of the rhombotin gene family that have oncogenic potential also encode LIM-containing proteins lacking homeodomains (McGuire et al., 1989; Boehm et al., 1990; Foroni et al., 1992).

In contrast with rhombotin and the LIM homeodomain proteins which are believed to be nuclear proteins (McGuire et al., 1991), two LIM domain proteins, zyxin and the cysteine-rich protein (CRP), have been detected in association with adhesion plaques and the actin cytoskeleton (Beckerle, 1986; Crawford & Beckerle, 1991; Crawford et al., 1992; Sadler et al., 1992). Interestingly, CRP expression is coordinate with c-Myc in response to serum induction and is suppressed in a variety of transformed cells, an observation consistent with the hypothesis that CRP is involved in the regulation of cell growth or differentiation (Wang et al., 1992; Weiskirchen & Bister, 1993). Thus, the LIM domain is found in a variety of proteins having distinct functions that are localized in distinct subcellular compartments.

The biochemical function of the LIM domain has not been ascertained. The discovery of LIM domains in both proteins that display and lack DNA-binding homeodomains led to the suggestion that the LIM domain might support protein–protein

† D.R.W. acknowledges support by grant (ES 03817) from the National Institute of Environmental Health Sciences, National Institutes of Health; M.C.B. acknowledges support from the American Heart Association and the National Institutes of Health (HL 41553). M.C.B. is an Established Investigator of the American Heart Association. The 500-MHz NMR facility was established in part by Grant RR5 06262 from the National Institutes of Health. J.W.M. was supported by Grant T35 HL07744 from the National Institutes of Health.

* To whom correspondence should be addressed. Telephone: 801-585-5103 (D.R.W.) or 801-581-4485 (M.C.B.); Fax: 801-585-5469 (D.R.W.) or 801-581-4668 (M.C.B.)

‡ Department of Medicine.

§ Department of Biochemistry.

∥ Department of Biology.

⊥ Department of Medicinal Chemistry.

® Abstract published in *Advance ACS Abstracts*, December 15, 1993.

0006-2960/94/0433-468$04.50/0 

interactions (Rabbitts & Boehm, 1990). Recent work supports this notion. For example, it has been demonstrated that two LIM proteins, zyxin and CRP, are colocalized in cells and can interact directly in vitro (Sadler et al., 1992). Moreover, deletion of the LIM domains of the Lmx-1 transcription factor eliminates its synergistic interaction with the helix–loop–helix transcription factor, Pan-1, without affecting the basal level of Lmx-1-dependent transcriptional activation (German et al., 1992). A plausible interpretation of this result is that the LIM domains of Lmx-1 mediate a direct or indirect interaction with Pan-1. Likewise, an oligomeric complex between Mec-3 and a POU homeodomain protein, Unc-86, appears to be important in the regulation of *mec-3* gene expression (Xue et al., 1993).

The number and spacing of cysteine and histidine residues in the LIM consensus sequence are reminiscent of a metal-binding motif. We demonstrated that the LIM domain protein CRP is a specific Zn-binding protein (Michelsen et al., 1993). A maximum of four Zn(II) ions are bound to CRP purified from avian muscle, suggesting that a single LIM domain is capable of binding two Zn(II) ions (Michelsen et al., 1993). We postulated that each LIM domain of CRP is comprised of a tetrathiolate $Cys_4$ Zn(II)-binding site and a $Cys_3His_1$ Zn(II) site. Analysis of zyxin purified from avian muscle also revealed the exclusive presence of bound Zn(II) ions (Sadler et al., 1992). No iron or copper was observed in either zyxin or CRP purified from their endogenous sources or from CRP isolated from a bacterial expression system, in support of the generalization that LIM domain proteins are specific Zn(II) metalloproteins (Sadler et al., 1992; Michelsen et al., 1993). Our finding that zyxin and CRP bind exclusively Zn(II) contrasts with a report that Lin-11 exhibits an iron–sulfur cluster in addition to Zn(II) (Li et al., 1991). Technical differences in the way the LIM proteins were prepared for metal analysis may account for the differences in the results. Whereas zyxin and CRP could be isolated from their endogenous source or from a bacterial expression system under nondenaturing conditions, the isolation of bacterially-expressed Lin-11 required extraction of the protein from insoluble inclusion bodies with urea.

The number of LIM domains present in a protein sequence varies from one to three. The majority of LIM proteins, including CRP, display two copies of the LIM motif. However, zyxin exhibits three C-terminal LIM domains and CRIP exhibits only a single LIM domain. The presence of multiple LIM domains in CRP compromised our study of the metal centers (Michelsen et al., 1993) as we were unable to focus on properties of a single domain. Toward the goal of understanding metal ion coordination within LIM domains, we sought to characterize metal centers in proteins containing a single LIM domain. Consequently, we have expressed and purified CRIP, the only protein known to contain a single LIM domain, as well as a single LIM domain derived from CRP for metal analysis. In this report we present the biophysical characterization of the metal centers in CRIP and the CRP truncate, designated LIM2. The results show that a common mode of metal ion coordination exists in these two molecules, suggesting that LIM domains present in different proteins may adopt a similar structural architecture.

## EXPERIMENTAL PROCEDURES

*Purification of CRIP.* The rat CRIP gene was amplified by RT/PCR from rat intestinal RNA using primers which engineered a *Nde*I restriction site containing the start codon and a *Bam*HI site downstream of the stop codon. The gene was cloned into the ATG site of the T7 expression vector pET-3a (Novagen), and DNA sequencing was carried out to confirm the CRIP sequence. The protein was expressed in BL21(DE3) cells also carrying the pLysS plasmid. Bacterial extracts were obtained by lysis of cells grown to logarithmic phase ($OD_{600nm}$ 0.5) and induced for 3 h with 0.4 mM IPTG in the presence of 0.2 mM $ZnSO_4$. The extract was cleared by high-speed centrifugation and applied to a CM-52 cation-exchange resin equilibrated in 10 mM potassium phosphate, pH 8. The protein was eluted with a 500-mL gradient of 0–250 mM KCl and pooled on the basis of absorbance at 280 nm and zinc concentration, as determined by atomic absorption spectroscopy. CRIP was concentrated by lyophilization and chromatographed on Sephadex G-50. The criteria used to establish sample purity were evidence of a single band on SDS–polyacrylamide gel electrophoresis and a single component by $C_{18}$ reverse-phase HPLC.

*Purification of LIM2.* The chicken CRP gene encodes a 192 amino acid protein with two LIM domains. To construct a plasmid for expression of a single LIM domain derived from CRP, we used PCR to amplify the sequences coding for Met-108 through the terminal Gln-192. The PCR primers incorporated an *Nde*I site around the start codon and a *Bam*HI site just downstream of the stop codon. The amplified DNA encodes approximately half of CRP including the C-terminal LIM domain and is referred to as LIM2. The LIM2 sequences were directionally cloned into the plasmid expression vector pAED4 (Doering and Matsudaira, unpublished results) which is a derivative of the T7-based expression vector, pET-3a (Studier et al., 1990). The authenticity of the expression plasmid, termed pAED4-LIM2, was confirmed by DNA sequence analysis.

For expression of LIM2 sequences in bacteria, pAED4-LIM2 was transformed into *E. coli* BL21(DE3). Cells grown to an $OD_{600nm}$ of 0.7–0.9 were induced to express the LIM2 protein by addition of 0.4 mM IPTG, and incubation was continued for 3 h at 37 °C. The cells were collected by centrifugation, were resuspended in ice-cold lysis buffer (10 mM KCl, 10 mM potassium phosphate, pH 7.2, 10 mM DTT; 20 mL of lysis buffer/L of cell culture), and were lysed by a freeze–thaw cycle followed by sonication. The lysate was cleared by centrifugation for 30 min at 12000*g*, and the resulting supernatant was equilibrated in 10 mM KCl, 10 mM potassium phosphate, pH 7.2, and 0.1% 2-mercaptoethanol and was then applied to a CM-52 cation-exchange column equilibrated in the same buffer. Elution of LIM2 was achieved with a linear gradient of 0–250 mM KCl in the column buffer. Fractions enriched in LIM2 were identified by SDS–polyacrylamide gel electrophoresis and were pooled. The protein was concentrated by lyophilization and chromatographed on Sephadex G-50 in 50 mM KCl, 20 mM potassium phosphate, and 1 mM DTT. Fractions containing LIM2 were pooled. The LIM2 protein was purified to apparent homogeneity by this method based on examination on SDS–polyacrylamide gel electrophoresis and amino acid analysis.

*Metal Ion Reconstitution.* Apoproteins were prepared by chromatography of $Zn_2$CRIP and $Zn_2$LIM2 on Sephadex G-25 equilibrated at pH 2. The Zn(II)-free proteins were found to contain reduced sulfhydryl groups. The concentration of each protein was quantified by amino acid analysis. Metal reconstitution was achieved by mixing the apoproteins in 0.025 N HCl with a set mole equivalency of metal ion followed by neutralization with Tris base to a specified pH. The metal stock solutions were made in 1 mM HCl, and concentrations

A

```
CRIP:   ..CPKCDKEVYFAERVTSLGKDWHRPCLKCEKCGKTLTSGGHAEHEGKPYCNHPC..
LIM-2:  ..CPRCGQAVYAAEKVIGAGKSWHKSCFRCAKCGKSLESTTLADKDGEIYCKGC..

LIM
Consensus:   CX2C.....X16-23.....HX2CX2CX2C.....X16-21.....CX2-3(C,H,D)

Consensus
Position:    1..2.................3..4..5..6.................7..8
```

B

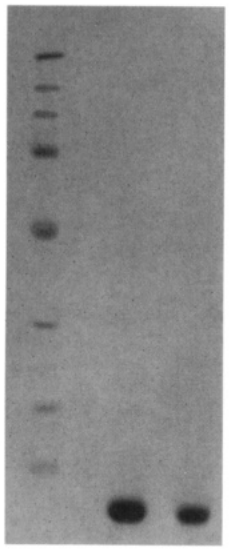


FIGURE 1: Partial sequence and purification of the CRIP and LIM2 proteins. (A) Comparison of the LIM domains of CRIP and LIM2. The LIM consensus sequence is derived from 19 LIM domains (Sadler et al., 1992). The eight positions that are highly conserved and are thought to be involved in metal coordination are indicated. (B) Coomassie blue-stained gel showing molecular mass markers (lane 1), purified CRIP (lane 2), and purified LIM2 (lane 3).

were verified by atomic absorption spectroscopy. Reconstitutions with Co(II) and Cu(I)–acetonitrile were carried out anaerobically.

*Spectroscopic Analyses.* Ultraviolet absorption spectroscopy was carried out on a Beckman DU spectrophotometer. Luminescence measurements were made on a Perkin-Elmer 650-10S fluorimeter. $^{113}Cd$ NMR spectroscopy was performed on a Unity 500 Varian spectrometer operating in the Fourier transform mode at 110.89 MHz. Spectra were recorded on $^{113}Cd$ samples (2–13 mg/mL) containing $^2H_2O$ as a field lock. The heteronuclear multiple quantum coherence (HMQC) spectra were recorded on the Unity 500 Varian spectrometer using the standard HMQC pulse sequence with solvent presaturation (Bax et al., 1983; Bax & Subramanian, 1983).

*Structural Probes.* Intrinsic fluorescence measurements were made on a Perkin-Elmer 650-10S fluorimeter. Circular dichroism studies were carried out on a Aviv 62DS spectrometer, with sample concentrations yielding absorbances of 0.8 at 220 nm in 0.1-cm cuvettes. Repetitive scans and postrun smoothing routines were used. Stokes' radii were determined by gel filtration on a Pharmacia FPLC Superdex 75 column equilibrated with 10 mM Tris-HCl, pH 7.4, containing 200 mM KCl. The proteins used to calibrate the column and the Stokes' radii used in the standard curve are ovalbumin (28 Å), trypsinogen (20.9 Å), ribonuclease (17.9 Å), cytochrome *c* (17 Å), and pancreatic trypsin inhibitor (13.4 Å). The Stokes' radii of standards were from published values (Le Maire et al., 1980, 1986; Tanford, 1961).

## RESULTS

*Purification of CRIP and LIM2.* Both CRIP and the LIM2 peptide derived from CRP display a single LIM domain (Figure 1A). CRIP was purified from bacteria induced with IPTG in the presence of 0.2 mM $ZnSO_4$. Purification was achieved by a combination of cation-exchange chromatography and gel filtration. Approximately 11 mg of CRIP was isolated per liter of culture. CRIP was shown to be homogeneous by the observation of a single band on SDS–polyacrylamide gel electrophoresis (Figure 1B, lane 2), a single symmetrical elution peak on $C_{18}$ reverse-phase HPLC, and the expected amino acid composition. The molecular mass determined by electrospray mass spectrometry of CRIP recovered from HPLC at pH 2 was 8419.7 daltons (Da). The mass as determined from the decoded DNA sequence was exactly 131 Da greater than the observed mass. The difference between the calculated and observed mass can be accounted for by the loss of the N-terminal Met (131.04 Da), leaving a protein of 76 residues. The Stokes' radius ($R$) of CRIP was found to be near 14.3 Å. The ratio of the observed Stokes' radius to the calculated $R_{min}$ of a sphere of $M_r$ 8419 was 1.06, implying that CRIP is monomeric and globular in shape.

LIM2 was purified from bacteria induced with IPTG in the presence or absence of 0.2 mM $ZnSO_4$. The purification protocol involved cation-exchange chromatography and gel filtration. We obtained 5–10 mg of purified LIM2/L of bacterial culture. The isolated LIM2 peptide appeared as a single band on SDS–polyacrylamide gels (Figure 1B, lane 3) and exhibited the expected amino acid composition. The molecular mass as determined from electrospray mass spec-

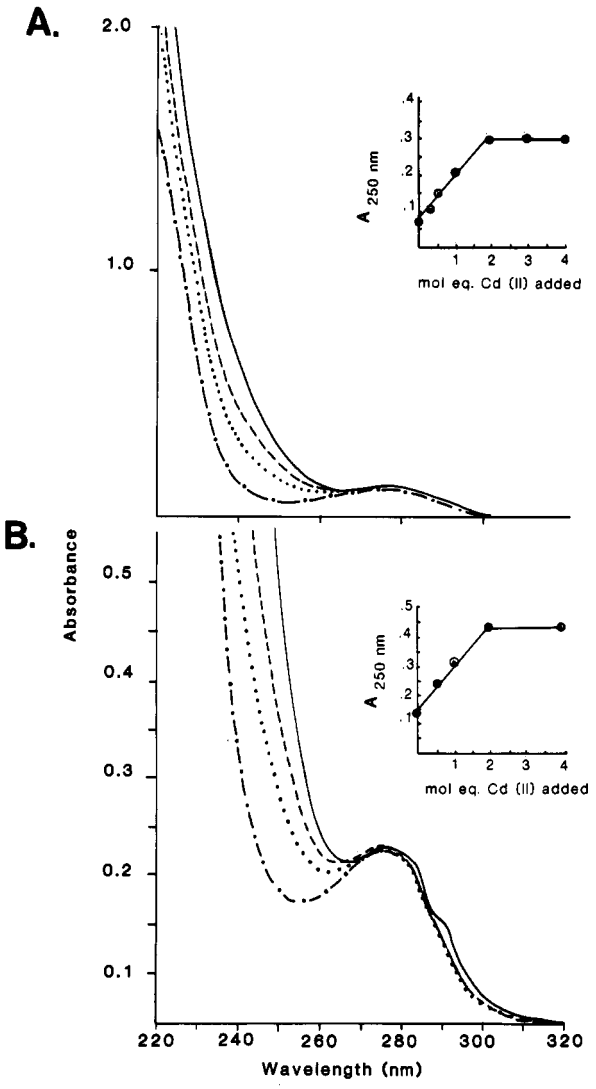


FIGURE 2: Ultraviolet absorption spectroscopy of CRIP (panel A) and LIM2 (panel B) titrated with increasing mole equivalency of Cd(II). Samples of apoproteins were reconstituted with Cd(II) as described in the Experimental Procedures to final stoichiometries of 0 (– • –), 0.5 (•••), 1.0 (- - -), 2.0 (—), 3.0, and 4.0 mol equiv. Samples reconstituted with 3 and 4 mol equiv of Cd(II) yielded spectra identical to those with 2 mol equiv Cd(II). The insets show the absorbance rise at 250 nm as a function of added Cd(II).

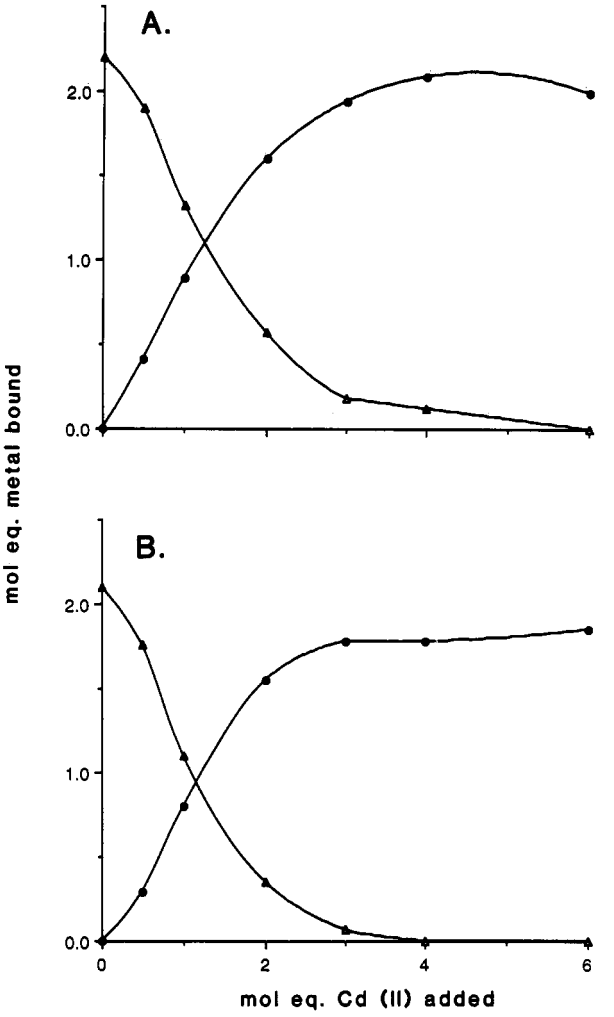


FIGURE 3: Displacement of protein-bound Zn(II) ions by exogenous Cd(II). Zn(II) complexes of CRIP (panel A) and LIM2 (panel B) were incubated for 3 h with increasing mole equivalency of Cd(II) at pH 7.5. Subsequently, the samples were dialyzed overnight in 40 mM Tris-HCl, pH 7.5, containing 40 mM KCl and quantified for metal and protein concentrations.

trometry of LIM2 was 8693.5 Da. As with CRIP, the observed mass was 131 Da less than that predicted from the decoded nucleotide sequence, indicating that the N-terminal Met was also processed in LIM2. The resulting polypeptide contains 84 residues. The Stokes' radius of LIM2 was 17.2 Å. The $R_{obs}/R_{min}$ ratio of 1.26 is indicative of a monomeric state with limited asymmetry in shape.

*Metal Content of CRIP and LIM2.* Both purified CRIP and LIM2 were found to contain 2.1 mol of Zn(II)/mol of protein. LIM2 was isolated as a Zn protein regardless of whether $ZnSO_4$ was added to the culture medium. No copper or iron was found in either purified sample.

Metal ion titration studies were carried out with CRIP and LIM2 to determine the maximal number of metal-binding sites. Both proteins were depleted of bound metal ions by gel filtration chromatography at pH 2. The metal-free proteins were stable, and the cysteinyl thiol groups were found to be totally reduced. Both proteins were titrated with increasing quantities of Cd(II), and the metal–ligand charge-transfer transitions in the ultraviolet were monitored by absorption spectrometry. The transitions were maximal at 2 mol equiv of added Cd(II) (Figure 2). Addition of Cd(II) in excess of 2 mol equiv did not alter the absorption spectrum of either CRIP or LIM2. Binding of 2 mol equiv of Cd(II) to each protein yielded a 295-nm shoulder in the aromatic peak. This tryptophan-related transition is seen only in fully metalated CRIP and LIM2 and is consistent with a more apolar environment in the fully metalated proteins.

To confirm that maximal binding occurred at 2 mol equiv, apo-CRIP was titrated with increasing quantities of Cd(II) from 0.5 to 4 mol equiv. The samples were initially dialyzed in buffer containing 0.1 mM 1,10-*o*-phenanthroline followed by extensive dialysis in buffer to remove any metal chelate. Cd(II) binding was maximal at 2 mol equiv even in samples reconstituted in the presence of 4 mol equiv of Cd(II). We showed previously that the maximal Zn or Cd binding by CRP was 4 mol equiv, consistent with a maximum of 2 metal-binding sites per LIM domain (Michelsen et al., 1993).

Addition of Cd(II) to $Zn_2$CRIP and $Zn_2$LIM2 resulted in a concentration-dependent displacement of bound Zn(II) ions (Figure 3). A nearly 1:1 stoichiometry in the Cd-induced Zn(II) displacement occurred between 0.5 and 1 mol equiv of added Cd(II). The displacement of the second bound Zn-(II) required higher concentrations of Cd(II). Neither protein

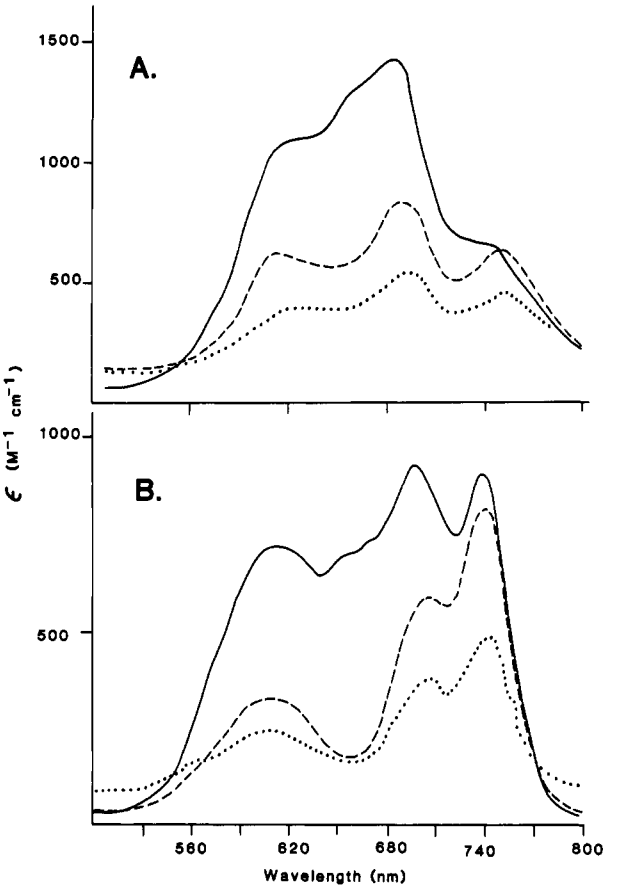


FIGURE 4: Electronic spectra of Co(II) complexes of CRIP (panel A) and LIM2 (panel B). Apoprotein samples were reconstituted with increasing mole equivalency of Co(II) under anaerobic conditions to final stoichiometries of 0.5 (···), 1.0 (- - -), 2.0 (—), and 3 mol equiv of Co(II). Samples with 3 mol equiv of Co(II) exhibited identical spectra to those of samples with 2 mol equiv of Co(II).

was fully depleted of bound Zn(II) during the time of the assay unless more than 3 mol equiv of Cd(II) was added.

Reconstitution of CRIP and LIM2 with Cu(I) stabilized as Cu(I)–acetonitrile resulted in luminescent Cu(I)–protein complexes. The emission is an indication of Cu(I) binding in a solvent-excluded environment (Beltramini et al., 1989). Titration of apoproteins with Cu(I) revealed maximal emission at 3 mol equiv of Cu(I) for each protein. Addition of Cu(I) in excess of 3 mol equiv resulted in a concentration-dependent diminution in emission consistent with disruption of the Cu(I) complex. Similar results were observed in studies in which Cu(I) was added to $Zn_2$CRIP and $Zn_2$LIM2 at neutral pH.

*Co(II) Complexes in CRIP and LIM2.* Apo-CRIP and apo-LIM2 were reconstituted with Co(II) to probe the environment of the two metal sites. Co(II) is frequently used as a spectroscopic probe of Zn(II) sites in metalloproteins (Bertini & Luchinat, 1984). Apo-CRIP and apo-LIM2 reconstituted anaerobically with increasing quantities of Co(II) yielded blue-green Co(II) complexes. The electronic spectra were dominated by d–d transitions that gained maximal intensity at 2 mol equiv of Co(II) (Figure 4). Three major transitions were observed with both samples, with maxima at 626 nm [$\epsilon$ = 539 $M^{-1}cm^{-1}$ per Co(II)], 688 nm ($\epsilon$ = 709), and 751 nm ($\epsilon$ = 326) for $Co_2$CRIP and maxima at 616 nm [$\epsilon$ = 358 $M^{-1}$ $cm^{-1}$ per Co(II)], 699 nm ($\epsilon$ = 463), and 741 nm ($\epsilon$ = 449) for $Co_2$LIM2. The energy of these transitions and the molar extinction coefficients are typical of $\nu_3[^4A_2 \rightarrow {}^4T_1(P)]$ transitions of four-coordinate high-spin Co(II) complexes having distorted tetrahedral coordination geometry (Bertini & Luchinat, 1984; Dance, 1979; Giedroc & Coleman,1986; Johnson & Schachman, 1983; Lane et al., 1977; May & Juo, 1978; Swenson et al., 1978). The molar extinction coefficients of the d–d transitions of tetrahedral Co(II) complexes is typically 300–1000 per Co(II) ion, and the centroid of the d–d $\nu_3$ envelope for $S_4$ and $N_4$ coordination is usually near 660 avd 550 nm, respectively (Bertini & Luchinat, 1984).

The electronic spectra of CRIP and LIM2 titrated with less than 2 mol equiv of Co(II) yielded a distinct envelope of transitions at both pH 7.5 and 8.5 (Figure 4). In each case the 740+-nm transition was more pronounced compared to that in $Co_2$CRIP and $Co_2$LIM2. The change in the d–d envelope of CoCRIP and CoLIM2 samples in going from 1 to 2 mol equiv is a clear indication of stepwise population of the two metal centers in both proteins.

All known LIM domain proteins exhibit eight spatially aligned potential metal ligands (Figure 1A). The eight conserved potential ligands in both CRP and CRIP include seven cysteines and one histidine. We previously reported electronic spectroscopy and $^{113}$Cd NMR studies on intact CRP demonstrating the presence of two tetrathiolate Zn(II) sites (Michelsen et al., 1993). The absolute conservation of a His in the central core of the motif in all LIM domain proteins suggested that the additional two Zn(II) sites in CRP were comprised of $Cys_3His_1$ ligands. The prominent 740+-nm component in the d–d bands of both $Co_1$LIM2 and $Co_1$CRIP (Figure 4) is consistent with tetrathiolate coordination for the first metal-binding site. Only proteins containing a tetrathiolate ($S_4$) site show any significant d–d transitions between 730 and 800 nm (Bertini & Luchinat, 1984). The ratio of the 740-nm component to the 680–700-nm component in the d–d envelope decreased with the binding of the second Co(II) ion to both CRIP and LIM2 (Figure 4). An imidazole ligand present in the second site is predicted to yield a dominant d–d transition near 680 nm (Bertini & Luchinat, 1984). The lowest energy component of the d–d envelope of Co(II) complexes with $S_3N_1$ ligands is near 700 nm (Fitzgerald & Coleman, 1991; Geidroc et al., 1992). Samples containing 2 mol equiv of Co(II) would be expected to yield an average d–d envelope with contributions from both sites as we observed for both CRIP and LIM2 (Figure 4). To obtain the d–d envelope of the candidate $S_3N_1$ site, apo-CRIP and apo-LIM2 samples were preformed with 1 mol equiv of Zn(II) followed by addition of 1 mol equiv of Co(II). Binding of $d_{10}$ Zn(II) to the $S_4$ site permitted analysis of the Co(II) d–d transitions at the candidate $S_3N_1$ site. The electronic spectra of these complexes were dominated by the 680–700-nm component, with only minor contributions from the 740+-nm transition (Figure 5, dotted lines). These spectra are consistent with the possible presence of a histidyl imidazole ligand. In this experiment, Zn(II) must be binding to the $S_4$ site as binding of the single Co(II) ion when added last did not yield the usual dominant 740-nm transition.

The two metal sites within an LIM domain exhibit different exchange rates. Samples of $Co_2$CRIP and $Co_2$LIM2 were incubated with 1 mol equiv of Zn(II) at neutral pH, and spectra were recorded anaerobically as a function of time after the addition of Zn(II). Addition of 1 mol equiv of Zn(II) to $Co_2$CRIP converted the electronic spectrum to one resembling $Co_1$CRIP, with the appearance of a distinct 750-nm transition (Figure 5A). The same was observed with LIM2 (Figure 5B). This indicates that the Co(II) in the second metal-binding site is kinetically more susceptible to displacement. The spectrum of $Zn_1Co_1$LIM2 samples with Co(II) in either site did not change over a 3-day period, suggesting that metal

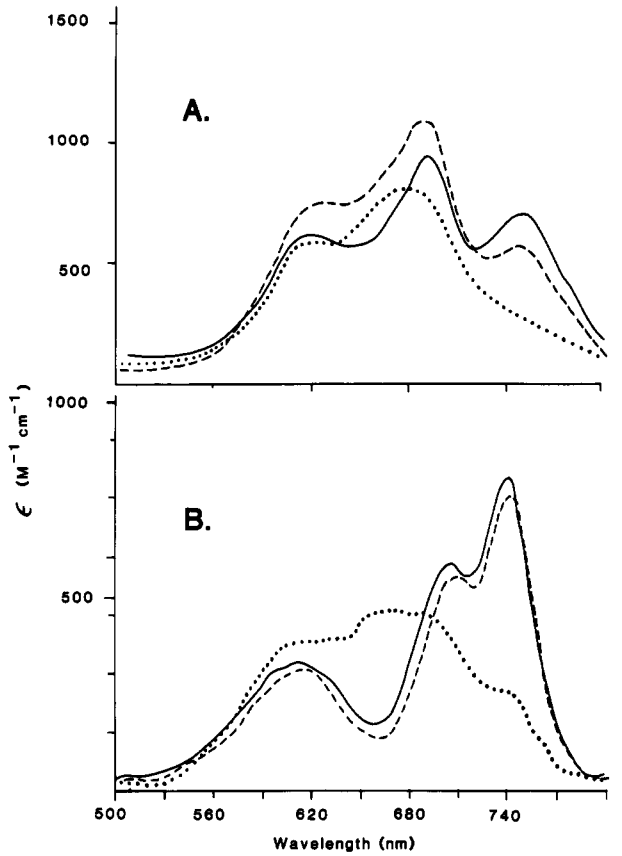


FIGURE 5: Electronic spectra of CRIP (panel A) and LIM2 (panel B) containing a single Co(II). The solid lines represent samples reconstituted with 1 mol equiv of Co(II). Dashed lines represent samples reconstituted with 2 mol equiv of Co(II) followed by the subsequent addition of 1 mol equiv of Zn(II) to samples at pH 8.5. Dotted lines represent samples reconstituted with 1 mol equiv of Zn(II) followed by the subsequent addition of 1 mol equiv of Co(II) after pH neutralization. The spectra shown were recorded within 1 h after the reconstitution procedure.

exchange between sites was minimal. In contrast, the spectrum of $Zn_1Co_1$CRIP samples changed appreciably with time in that the 750-nm transition diminished in intensity and a 560-nm transition intensified consistent with slow exchange of the Zn(II) and Co(II) ions between the two sites (data not shown). There was no indication of Co(II) oxidation during that time period in either sample. Addition of 2 mol equiv of Zn(II) to $Co_2$LIM2 abolished the observed d–d transitions.

*$^{113}$Cd NMR of CRIP and LIM2.* $^{113}$Cd NMR was carried out with both LIM2 and CRIP (Figure 6). NMR of apo-LIM2 reconstituted with 2 mol equiv of $^{113}$Cd(II) revealed two resonances at 707 and 648 ppm relative to $Cd(ClO_4)_2$ (Figure 6B). We previously reported $^{113}$Cd NMR data of the LIM2 parent molecule, CRP, in which two resonances at 707 and 646 ppm were observed in $^{113}Cd_4$CRP (Michelsen et al., 1993). The observation of only two signals in $Cd_4$CRP was interpreted as showing similar metal ion environments in the two LIM domains of CRP. The fact that $Cd_2$LIM2 exhibits the same $^{113}$Cd chemical shifts as the fully metalled CRP is consistent with that interpretation and furthermore is indicative that the LIM2 protein adopts a native fold. The $^{113}$Cd signal at 707 ppm is consistent with tetrathiolate coordination, whereas the assignment of the ligands for the site exhibiting a $^{113}$Cd signal at 648 ppm is ambiguous and could represent either an $S_4$ site or an $S_3N_1$. Measurement of the $T_1$ for the two signals yielded values of 0.8 and 0.2 s for the 707 and 648 ppm signals, respectively.

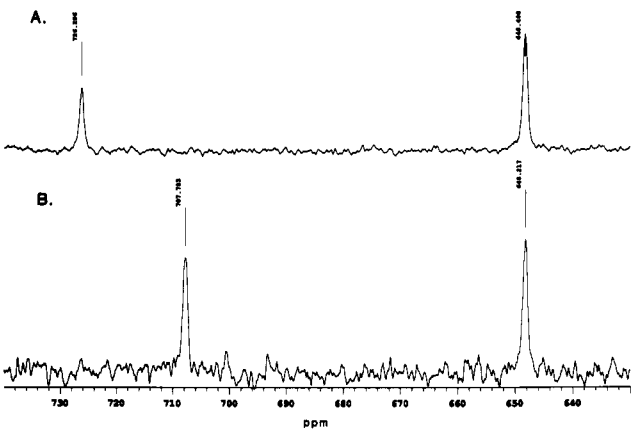


FIGURE 6: $^{113}$Cd NMR of CRIP (panel A) and LIM2 (panel B). $^{113}Cd_2$CRIP and $^{113}Cd_2$LIM2 samples were analyzed by NMR spectroscopy. Samples of $Cd_2$CRIP and $Cd_2$LIM2 at pH 7.4 were concentrated by ultrafiltration on an Amicon YM3 membrane to final concentrations near 13 and 8 mg/mL, respectively. Chemical shifts are relative to 1 M $Cd(ClO_4)_2$. The number of transients was 19 000 and 7500 for CRIP and LIM2, respectively. Samples contained $^2H_2O$ as a field lock. Parameters used include a spectral width of 22.1 kHz, an acquisition time of 0.8 s, and a pulse width of 60°. A 40-Hz line broadening was applied for spectral enhancement.

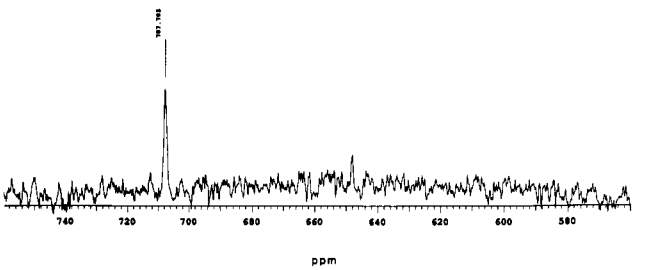


FIGURE 7: $^{113}$Cd NMR of monometalated LIM2. Apo-LIM2 (8 mg/mL) was reconstituted with 1 mol equiv of $^{113}$Cd(II) and analyzed by NMR spectroscopy under similar conditions specified in the legend to Figure 6. The number of transients was 8128.

$^{113}$Cd NMR of $Cd_2$CRIP revealed two resonances at 726 and 648 ppm (Figure 6A). The 648 ppm signal had approximately twice the intensity of the $^{113}$Cd signal at 726 ppm when the relaxation delay was set at 0.8 s. The difference in amplitude between the two signals is accounted for by differences in $T_1$ of the two $^{113}$Cd nuclei. The $T_1$'s were measured by inversion–recovery and found to be 2.3 s for the 726 ppm peak and 0.3 s for the 648 ppm signal.

As discussed above, spectroscopy of Co(II) complexes of CRIP and LIM2 suggested that Co(II) binding at the $S_4$ site is kinetically and thermodynamically preferred. Since the $S_4$ site clearly yields the downfield $^{113}$Cd signal, the prediction was that monometalated complexes of $^{113}Cd_1$CRIP and $^{113}Cd_1$-LIM2 would show a predominant 700+ ppm signal. To test this prediction, apo-LIM2 was reconstituted with 1 mol equiv of $^{113}$Cd(II). After neutralization of the sample 1 mol equiv of Zn(II) was added to form a $^{113}Cd_1Zn_1$LIM2 complex. NMR of this complex revealed signals at 707 and 648 ppm, with the 707 ppm component being at least 3-fold greater in intensity (Figure 7). These results support the interpretation that the $S_4$ site is the preferred, initial site of metal ion binding. Although spectroscopic data of $Co_1$CRIP showed metal binding predominantly within the $S_4$ site, NMR of $^{113}Cd_{0.5}$-CRIP showed two signals with the same chemical shift as observed in $^{113}Cd_2$CRIP and only a slightly greater intensity observed in the 726 ppm signal when the different $T_1$ values are considered (data not shown). It is unclear whether the

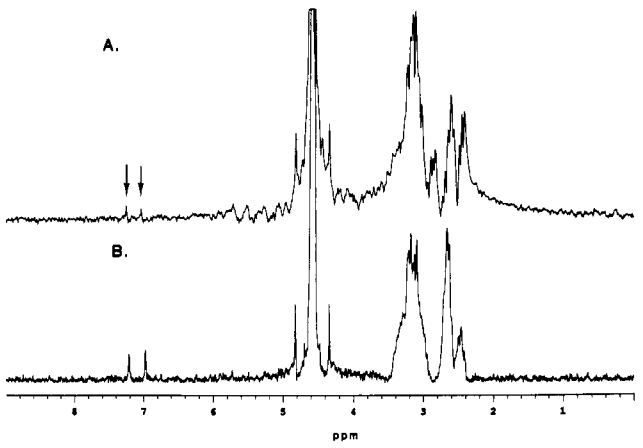


FIGURE 8: Heteronuclear multiple quantum coherence NMR of $^{113}Cd_2$CRIP (panel A) and $^{113}Cd_2$LIM2 (panel B). The one-dimensional $^1H$–$^{113}Cd$ multiple quantum filtered proton NMR spectrum was acquired using a standard HMQC pulse sequence (Bax et al., 1986). The $1/(2J)$ delay was set at 8 ms. The arrows show the positions of the H2 and H4 ring protons of His.

presence of two $^{113}Cd$ signals in $Cd_{0.5}$CRIP arises from kinetic or thermodynamic influences.

Thus far, it has been impossible to assign the ligands for the 648 ppm signal in $^{113}Cd$(II) complexes of CRIP and LIM2 without some ambiguity. There is precedent for both $S_4$ and $S_3N_1$ sites showing $^{113}Cd$ signals with chemical shifts between 630 and 660 ppm (Fitzgerald & Coleman, 1991; Giedroc et al., 1992; Pan & Coleman, 1990). Therefore, to test directly whether the conserved His is a metal ligand, we performed $^1H$–$^{113}Cd$ heteronuclear multiple quantum correlation (HMQC) NMR. This experiment has been successfully used to assign amino acid side chains that ligate metal ions (Live et al., 1985; South et al., 1989). In HMQC NMR only $^1H$ signals of protons that are scalar coupled to the $^{113}Cd$ nuclei are observed. The $^1H$–$^{113}Cd$ scalar coupling experiment exhibited signals in the spectral region where the His-H2 and His-H4 ring protons (7.2 and 7 ppm, respectively) appear. In addition, signals between 2.5 and 3.5 ppm were observed, consistent with scalar coupling to $\beta$-protons of cysteines (Figure 8). The signals at 7.2 and 7 ppm are unambiguous evidence that a histidyl imidazole is a ligand to a $^{113}Cd$ nucleus. These protons must be scalar coupled to the 648 ppm $^{113}Cd$ nuclei in each protein. In the 500-MHz $^1H$ NMR spectrum of $Cd_2$-CRIP and $Cd_2$LIM2 protons are seen at 7.2 and 7 ppm. In addition, a wide dispersion of peptide amide protons was observed, implying a compact tertiary fold.

*Effect of Metal Ions on the Structures of CRIP and LIM2.* Bulk structural probes were used to determine the role of metal ions in the structures of CRIP and LIM2. Measurements of intrinsic fluorescence, hydrodynamic radii, and far-ultraviolet circular dichroism were made from protein samples with and without bound metal ions. Both CRIP and LIM2 contain a single tryptophan residue which resides in a sequence position adjacent to the conserved histidine in the LIM consensus sequence. The conserved His is the candidate imidazole ligand for the $S_3N_1$ site in LIM domain proteins. We found that Trp emission was a useful indicator of the dependency of protein structure on metal site occupancy. Native $Zn_2$CRIP exhibits a Trp emission maximum near 334 nm, which is indicative of a hydrophobic environment for the Trp residue. In the absence of bound Zn(II) or Cd(II) ions the Trp fluorescence in CRIP is red-shifted to 354 nm, which is consistent with an aqueous environment of the Trp residue. Emission measurements were made on apo-CRIP samples

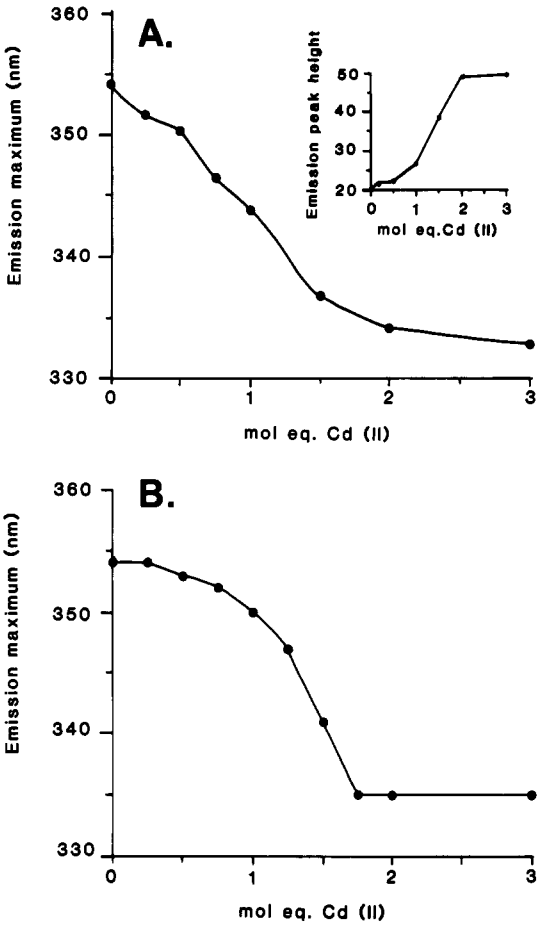


FIGURE 9: Intrinsic fluorescence of CRIP (panel A) and LIM2 (panel B) reconstituted with increasing quantities of Cd(II). The wavelength maximum of emission is plotted as a function of metal added to the two proteins. The relative quantum yield of the tryptophan fluorescence changed in CRIP with different stoichiometries of metal bound. The inset in panel A represents the relative amplitude of the emission of CRIP as a function of the quantity of bound Cd(II) ions.

titrated with increasing quantities of Cd(II). Metal binding to apo-CRIP blue-shifted the emission maximum, with the shift terminal at 334 nm with 2 mol equiv of Cd(II) (Figure 9A). The relative quantum yield of emission increased upon metal binding in an apparent biphasic manner (Figure 9A, inset). The change was modest in going from 0 to 1 mol equiv but dramatic in progressing from 1 to 2 mol equiv of Cd(II). The energy of Trp emission in LIM2 was also dependent on occupany of the metal-binding sites (Figure 9B). In the absence of metal, emission was maximal at 354 nm, implying that the Trp residue is exposed to an aqueous environment. Titration of apo-LIM2 with increasing quantities of Cd(II) resulted in a blue shift in emission toward 335 nm consistent with movement of the Trp residue to a more hydrophobic environment. The blue shift was minimal upon occupancy of the first binding site (354 to 350 nm) but shifted appreciably upon occupancy of the second site (350 to 335 nm) (Figure 9B). The biphasic change in the energy shift supports the conclusion from Co(II) titration studies that metal binding is a stepwise process in the LIM2 population, with one metal site being fully occupied prior to incorporation of metal into the second site.

The dependency of the tertiary folds of CRIP and LIM2 on metal binding was also demonstrated by measurement of Stokes' radii by size permeation chromatography (Table 1). The Stokes' radius of $Zn_2$CRIP and $Cd_2$CRIP was 14.3 ± 0.1 Å. The hydrodynamic radius increased to 16.8 Å upon metal

Table 1: Stokes' Radii of CRIP and LIM2 Proteins[a]

| sample | $R_{obs}$ (Å) | $R_{obs}/R_{min}$ | sample | $R_{obs}$ (Å) | $R_{obs}/R_{min}$ |
|---|---|---|---|---|---|
| native $Zn_2$-CRIP | 14.3 ± 0.1 | 1.06 | native $Zn_2$-LIM2 | 17.3 ± 0.1 | 1.26 |
| $Cd_2$CRIP | 14.3 ± 0.1 | 1.06 | $Cd_2$LIM2 | 17.2 ± 0.1 | 1.26 |
| $Cd_1$CRIP | 15.3 ± 0.1 | 1.13 | $Cd_1$LIM2 | 17.7 ± 0.1 | 1.29 |
| apo-CRIP | 16.8 ± 0.1 | 1.24 | apo-LIM2 | 18.4 ± 0.1 | 1.34 |
| $Cu_3$CRIP | 15.9 ± 0.1 | 1.17 | $Cu_3$LIM2 | 18.4 ± 0.1 | 1.34 |

[a] Stokes' radii were determined from size permeation chromatography on a Superdex 75 column equilibrated with 10 mM Tris-HCl, pH 7.4, containing 200 mM KCl. The minimal radii ($R_{min}$) calculated for CRIP and LIM2 assuming a sphere were 13.58 and 13.72, respectively. Each value of $R_{obs}$ is the mean of three independent runs.

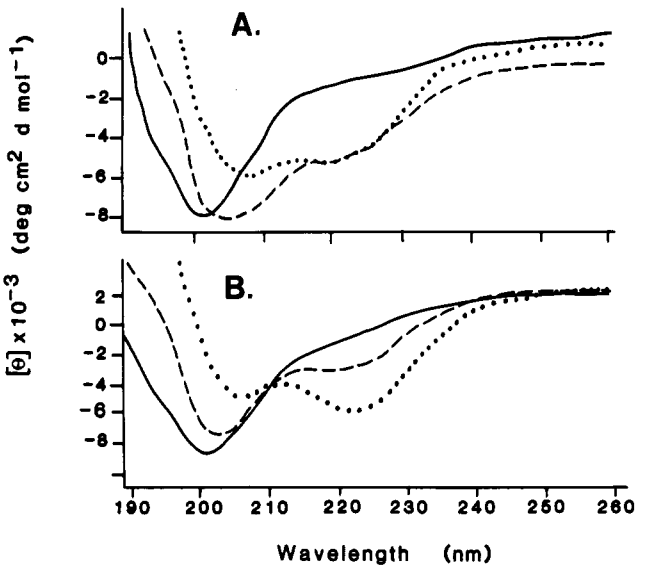


FIGURE 10: Circular dichroism of CRIP (panel A) and LIM2 (panel B) as a function of the quantity of bound Zn(II) ions. The ellipticity spectra of apoproteins (—) and proteins with either 1 mol equiv (- - -) or 2 mol equiv (···) bound Zn(II) ions were measured with 0.1-cm path length and at protein concentrations yielding an absorbance of nearly 0.8 at 220 nm. The spectra represent an average of 9 scans with a bandwidth of 0.7 nm. Each sample was in 50 mM potassium phosphate, pH 8.

depletion. A single symmetrical elution peak was observed for monometalated CRIP, correlating to a Stokes' radius of 15.3 Å. Occupancy of the binding sites with Cu(I) altered the hydrodynamic properties of CRIP. The observed Stokes' radius of either $Cu_{1.5}$CRIP or $Cu_3$CRIP was 15.9 Å.

The Stokes' radius of LIM2 increased from 17.3 to 18.4 Å upon depletion of metal ions, consistent with unfolding of the structure (Table 1). Binding of 2 mol equiv of Zn(II) to apo-LIM2 converted the radius back to 17.2 Å. As with CRIP, Cu(I) binding to LIM2 formed a complex with a hydrodynamic radius closer to that of the apoprotein, consistent with an elongated structure ($R_{obs}/R_{min}$ = 1.3). The Stokes' radius of $Zn_2$LIM2 was significantly higher than that of $Zn_2$CRIP (17.3 versus 14.3 Å), consistent with greater asymmetry in shape in LIM2. These differences could reflect the sequence heterogeneity outside the LIM domain. Chromatography of a mixture of the two Zn(II) proteins resolved the two components, with the expected elution profile for each protein.

Circular dichroism (CD) studies demonstrated that the secondary structures of both molecules are dependent on bound Zn(II) or Cd(II) ions (Figure 10). The addition of either Zn(II) or Cd(II) increased the negative ellipticity of CRIP and LIM2, consistent with gain of secondary structure. The similarity in ellipticity in Zn(II) and Cd(II) samples between 210 and 230 nm was indicative that the observed ellipticity was not due to chirality of the metal centers. Computer analysis of the CD spectra of metalated CRIP and LIM2 suggested predominantly $\beta$-structure in both proteins. Binding of Cu(I) by CRIP or LIM2 did not yield the same ellipticity pattern, suggestive that the Cu(I) conformer of each protein was distinct from the Zn(II)-induced conformer.

## DISCUSSION

CRIP and the C-terminal half of CRP (LIM2) each display a single LIM domain with highly similar metal coordination properties. By aligning the sequences of CRIP and LIM2 with respect to the conserved Cys residues in the LIM consensus sequence, it is apparent that the two proteins share 28 sequence identities out of 77 possible positions for a 36% sequence identity. In comparison, the N-terminal half of CRP is 51% identical to the C-terminal half (LIM2). Both CRIP and LIM2 exhibit a maximum of two Zn(II) per domain. Both proteins have the same tetrahedral symmetry around the divalent metal sites. Both CRIP and LIM2 have a similar ligand field pattern of one tetrathiolate ($S_4$) site and one $S_3N_1$ site for the divalent metal ions. $^{113}$Cd NMR of CRIP and LIM2 revealed a similar $^{113}$Cd chemical shift for the $S_3N_1$ sites in the two proteins, implying that the $^{113}$Cd nucleus is in a similar environment in the two proteins. $^{113}$Cd(II) bound to the $S_4$ site in CRIP exhibited a more downfield shift relative to the $S_4$ site in LIM2.

The two $^{113}$Cd chemical shifts in LIM2 were nearly identical to $^{113}$Cd chemical shifts in the intact CRP protein which displays two LIM domains. This result illustrates that the LIM2 fragment adopts a conformation with metal site environments comparable to the LIM domains studied in the context of intact CRP. The two LIM domains in CRP must therefore exist within independently folded segments of the CRP molecule.

Metal binding to the two sites within the LIM domain is sequential, with population of the $S_4$ site being kinetically preferred to binding at the $S_3N_1$ site. This was shown by Co(II) titration studies, $^{113}$Cd NMR spectroscopy, and intrinsic fluorescence measurements. Two types of metal exchange are observed. First, limited metal exchange occurs between the two sites within the LIM domain of CRIP and to a lesser extent in LIM2. From results with Co(II) spectroscopy and $^{113}$Cd NMR spectroscopy it is likely that different exchange rates exist between sites for different metal ions. Second, metal exchange with exogenous metals occurs, with the $S_3N_1$ site being kinetically more labile than the $S_4$ site. The observed facile metal exchange may imply that the thiolates in the $S_3N_1$ sites are more solvent-accessible. Solvent-accessible thiolates have been suggested to be important in the facile metal exchange known to occur in metallothionein (Otvos et al., 1989; Robbins et al. 1991), the significance of metal exchange in these proteins is unclear. Curiously, CRIP was reported to be important in intestinal metal ion transport by virtue of radiozinc binding when mucosal cells were bathed in medium containing $^{65}$Zn(II) (Hempe & Cousins, 1991). If CRIP is a Zn(II) transporter, metal exchange may be important in the function. Alternatively, one may account for the observations in the Hempe and Cousins report by the metal exchange properties of CRIP. Addition of radiozinc would be expected to result in labeling of CRIP at the $S_3N_1$ site, but the binding may not imply any physiological role in Zn(II) transport. The structures of both CRIP and LIM2 are metal-stabilized. In the absence of metal binding both proteins appear to be substantially unfolded. Apo-CRIP and

apo-LIM2 exhibit larger Stokes' radii, show less secondary structure by circular dichroism compared to the metalated proteins, and have the single Trp residue exposed to an aqueous environment. The tertiary folds of CRIP and LIM2 are dependent on the metal ion bound. Zn(II) induces a distinct fold compared to that induced by Cu(I). Cu(I) binds to both proteins, but the complexes exhibit a maximal Cu(I) stoichiometry of three. The dynamics of metal-induced structure may be of significance in function.

The similar metal coordination properties of CRIP and LIM2 may translate into a common structural architecture. The ligand fields of the two sites are similar. The $S_3N_1$ sites in both proteins exhibit a similar NMR $T_1$ value of 0.2 s. Fast relaxation at the $S_3N_1$ site may imply greater conformational flexibility at this site. A dynamic local conformation may also contribute to the facile metal exchange occurring at the $S_3N_1$ site.

It is now reasonable to postulate that the eight conserved residues in a LIM domain constitute the eight ligands for the two sites. For LIM2 and CRIP the eight conserved residues include seven Cys residues and one His residue (Figure 1A). In other LIM proteins the candidate ligand in the eighth consensus sequence position is often a His or Asp rather than Cys, consistent with the LIM consensus sequence: $C^1$-$X_2$-$C^2$-$X_{16-23}$-$H^3$-$X_2$-$C^4$-$X_2$-$C^5$-$X_2$-$C^6$-$X_{16-21}$-$C^7$-$X_{2-3}$-(C,H,D)[8] (superscipt numbering refers to candidate ligands, see Figure 1A). At this time there are no direct experimental data to indicate which of the conserved Cys residues constitute the tetrathiolate site. A number of alternatives are theoretically possible. For example, the LIM domain has been postulated to be a variant of a Zn finger with adjacent fingers (Wang et al., 1992). Tandemly arrayed Zn fingers are frequently observed in sequences containing the "classical Zn finger" sequence motif. Such a "double finger" structure could result if ligand residues 1–4 form the $S_3N_1$ site and residues 5–8 form the $S_4$ site in both LIM2 and CRIP. It is also possible that consensus residues 1, 2, 5, and 6 cooperate to establish the $S_4$ site, with residues 3, 4, 7, and 8 generating the $S_3N_1$ site. Another alternative arrangement of ligands could generate the $S_3N_1$ site with the centrally clustered ligands, residues 3–6, and the tetrathiolate site with residues 1, 2, 7, and 8. This structure would necessiate the polypeptide chain to fold back on itself, creating the $S_4$ site with the chain termini. There is no compelling reason to favor one model over the others.

If a common structural architecture exists between CRIP and LIM2, it is conceivable that a common motif will extend to all LIM domain proteins. All known LIM proteins, apart from CRIP, contain at least two tandemly repeated LIM domains, so a LIM domain may constitute a common substructural motif.

## ACKNOWLEDGMENT

The authors thank Jeffrey Cronk for construction of the LIM2 expression vector, Don Doering and Paul Matsudaira for providing the plasmid expression vector (pAED4), Mike Summers for advice on the heteronuclear multiple quantum correlation NMR experiment, Jim McCloskey for electrospray mass spectrometry, and Tom Alber for helpful discussions.

## REFERENCES

Bax, A., & Subramanian, S. (1986) *J. Magn. Reson. 67*, 565–569.

Bax, A., Griffey, R. H., & Hawkins, B. L. (1983) *J. Magn. Reson. 55*, 3012–3015.

Beckerle, M. C. (1986) *J. Cell Biol. 103*, 1679–1687.

Beltramini, M., Giacometti, G. M., Salvato, B., Giacometti, G., Munger, K., & Lerch, K. (1989) *Biochem. J. 260*, 189–193.

Bertini, I., & Luchinat, C. (1984) *Adv. Inorg. Biochem. 6*, 72–111.

Birkenmeier, E. H., & Gordon, J. I. (1986) *Proc. Natl. Acad. Sci. U,S,A, 83*, 2516–2520.

Boehm, T., Greenberg, J. M., Buluwela, L., Lavenir, I., Forster, A., & Rabbitts, T. H. (1990) EMBO J. 9, 857–868.

Bourgouin, C., Lundgren, S. E., & Thomas, J. B. (1992) *Neuron 9*, 549–561.

Cohen, B., McGuffin, E., Pfeifle, C., Segal, D., & Cohen, S. M. (1992) *Genes Dev. 6*, 715–729.

Crawford, A. W., & Beckerle, M. C. (1991) *J. Biol. Chem. 266*, 5847–5853.

Crawford, A. W., Michelsen, J. M., & Beckerle, M. C. (1992) *J. Cell Biol. 116*, 1381–1393.

Dance, I. G. (1979) *J. Am. Chem. Soc. 101*, 6264–6273.

Fitzgerald, D. W., & Coleman, J. E. (1990) *Biochemistry 30*, 5195–5201.

Foroni, L., Boehm, T., White, L., Forster, A., Sherringon, P., Liao, X. B., Brannan, C. I., Jenkins, N. A., Copeland, N. G., & Rabbits, T. H. (1992) *J. Mol. Biol. 226*, 747–761.

Freyd, G., Kim, S. K., & Horvitz, R. (1990) *Nature 344*, 876–879.

German, M. S., Wang, J., Chadwick, R. B., & Rutter, W. J. (1992) *Genes Dev. 6*, 2165–2176.

Giedroc, D. P., & Coleman, J. E. (1986) *Biochemistry 25*, 4969–4978.

Giedroc, D. P., Qui, H., Khan, R., King, G. C., & Chen, K. (1992) *Biochemistry 31*, 765–774.

Hempe, J. M., & Cousins, R. J. (1991) *Proc. Natl. Acad. Sci. U.S.A. 89*, 9671–9674.

Johnson, R. S., & Schachman, H. K. (1983) *J. Biol. Chem. 258*, 3528–3538.

Karlsson, O., Thor, S., Norberg, T., Ohlsson, H., & Edlund, T. (1990) *Nature 344*, 879–882.

Lane, R. W., Ibers, J. A., Frankel, R. B., Papaefthymiou, G. C., & Holm, R. H. (1977) *J. Am. Chem. Soc. 99*, 84–97.

LeMaire, M., Rivas, E., & Moller, J. V. (1980) *Anal. Biochem. 106*, 12–21.

LeMaire, M., Aggerbeck, L. P., Monteilhet, C., Andersen, J. P., & Moller, J. V. (1986) *Anal. Biochem. 154*, 525–535.

Li, P. M., Reichert, J., Freyd, G., Horvitz, H. R., & Walsh, C. T. (1991) *Proc. Natl. Acad. Sci. U.S.A. 88*, 9210–9213.

Liebhaber, S. A., Emery, J. G., Urbanek, M., Wang, X., & Cooke, N. E.(1990) *Nucleic Acids Res. 18*, 3871–3879.

Live, D. H., Kojiro, C. L., Cowburn, D., & Marklely, J. L. (1985) *J. Am. Chem. Soc. 107*, 3043–3045.

May, S. W., & Juo, J. Y. (1978) *Biochemistry 17*, 3333–3338.

McGuire, E. A., Hockett, R. D., Pollack, K. M., Bartholdi, M. F., O'Brien, S. J., & Korsmeyer, S. J. (1989) *Mol. Cell Biol. 9*, 2124–2132.

McGuire, E. A., Davis, A. R., & Korsmeyer, S. J. (1991) *Blood 77*, 599–606.

Michelsen, J. W., Schmeichel, K. L., Beckerle, M. C., & Winge, D. R. (1993) *Proc. Natl. Acad. Sci. U.S.A. 90*, 4404–4408.

Otvos, J. D., Petering, D. H., & Shaw, C. F. (1989) *Comments Inorg. Chem. 9*, 1–35.

Pan, T., & Coleman, J. E. (1990) *Biochemistry 29*, 3023–3029.

Rabbit, T. H., & Boehm, T. (1990) *Nature 346*, 418.

Robbins, A. H., McRee, D. E., Williamson, M., Collett, S. A., Xuong, N. H., Furey, W. F., Wang, B. C., & Stout, C. D. (1991) *J. Mol. Biol. 221*, 1269–1293.

Sadler, I., Crawford, A. W., Michelsen, J. W., & Beckerle, M. C. (1992) *J. Cell Biol. 119*, 1573–1587.

South, T. L., Kim, B., & Summers, M. F. (1989) *J. Am. Chem. Soc. 111*, 3395–3396.

Studier, F. W., Rosenberg, A. H., Dunn, J. J., & Dubendoff, J. W. (1990) *Methods Enzymol. 185*, 60–89.

Swenson, D., Baenziger, N. C., & Coucouvanis, D. (1978) *J. Am. Chem. Soc. 100*, 1932–1934.

Taira, M., Jamrich, M., Good, P. J., & Dawid, I. B. (1992) *Genes & Dev. 6*, 356–366.
Tanford, C. (1961) in *Physical Chemistry of Macromolecules*, John Wiley & Sons, New York.
Wang, X., Lee, G., Liebhaber, S. A., & Cooke, N. E. (1992) *J. Biol. Chem. 267*, 9176–9184.
Way, J. C., & Chalfie, M. (1988) *Cell 54*, 5–16.
Weiskirchen, R., & Bister, K. (1993) *Oncogene 8*, 2317–2324.
Xu, Y., Baldassare, M., Fisher, P., Rathbun, G., Oltz, E. H., Yancopoulos, G. D., Jessell, T.M., & Alt, F. W. (1993) *Proc. Natl. Acad. Sci. U.S.A. 90*, 227–231.
Xue, D., Tu, Y. & Chalfie, M. (1993) *Science 261*, 1324–1328.